Hierarchical Structure Gradients Developed in Injection-Molded PVDF and PVDF–PMMA Blends. I. Optical and Thermal Analysis

Y. D. WANG,* M. CAKMAK

Polymer Engineering Institute, College of Polymer Engineering and Polymer Science, University of Akron, Akron, Ohio 44325-0301

Received 5 December 1996; accepted 22 September 1997

ABSTRACT: The structural gradients developed along and across the flow direction of injection-molded PVDF and PVDF/PMMA parts were investigated by optical microscopy and thermal analysis techniques. The spatial variation of crystallinity across the thickness direction was found to be insensitive to the process variables: injection speed and mold temperature. This relatively flat crystallinity profile across the thickness of the parts was found to decrease with the increase of PMMA concentration. The blends become noncrystallizable beyond about 40–45% PMMA concentration. The influence of flow history on the structural evolution across the thickness was observed in the peak position of the cold crystallization region. This peak temperature showed a minimum at depths where shear effects are at their maximum. This was attributed to the increased levels of chain orientation frozen in the amorphous portions of these regions which crystallize at lower temperatures upon heating. © 1998 John Wiley & Sons, Inc. J Appl Polym Sci 68: 909–926, 1998

Key words: thermal analysis; polymer blends; processing effects; structure development

INTRODUCTION

The injection-molding process imposes complex thermal and stress effects on the produced parts. This is partly as a result of experiencing complex flow history by the polymer chains during their passage through sprue-runner-gate–cavity system and partly as a result of rapid cooling that they experience during this flow and subsequent holding stage. Because of the presence of highly directional stress and thermal gradients, the resulting part generally possess highly anisotropic properties due to complicated and heterogeneous structural features. Thus, the structural characterization of the injection-molded parts is essential in understanding the detailed mechanisms that occur during the course of this process. This will, in turn, ultimately help us in building a quantitative structure-based model.

Since its discovery, poly(vinylidene fluoride) (PVDF) has been the center of scientific attention in polymer science. However, among the large number of articles published, only a few covered the injection molding of PVDF[1,2] and blends[3] of PVDF with poly(methyl methacrylate) (PMMA). There is no detailed study involving structure development and its relation with processing conditions and resulting properties.

The present study is concerned with the influence of processing conditions on the development of structural hierarchy in injection-molded PVDF and blends of PVDF with PMMA. In order to obtain a quantitative understanding of the struc-

* *Present address:* DSM TPE's Inc., Leominster, Massachusetts 01453.

Correspondence to: M. Cakmak.

Contract grant sponsor: NSF DDM; contract grant number: 8858303.

Journal of Applied Polymer Science, Vol. 68, 909–926 (1998)
 CCC 0021-8995/98/060909-18

Table I Compositions of the Blends Prepared

Blend	Concentration (PVDF–PPMMA Wt %)
PVDF–PMMA	100/0, 85/15, 70/30, 55/45, 40/60, 20/80, 0/100

tural hierarchy and its three-dimensional spatial gradients developed under stress and thermal history during the processing, a wide range of structural characterization techniques need to be used. The acquired data need then be synthesized into one large composite hierarchical picture. For this purpose, many techniques were used in this study, including optical microscopy, differential scanning calorimetry, matrixing microbeam wide-angle X-ray diffraction, Fourier transform infrared spectroscopy, and small-angle X-ray scattering. Other techniques, such as microbeam small-angle light scattering and microbeam wide-angle X-ray pole figure, were also developed to determine the size and the shape of the spherulites and the orientation distribution of the injection-molded samples. These results are to be published in companion articles. In this article, we will present our experimental results obtained from the optical microscopy and thermal analysis.

EXPERIMENTAL

Materials

Poly(vinylidene fluoride) (PVDF; Kynar 720) was provided by Atochem. Its number- and weight-average molecular weights measured using the gel permeation chromatography (GPC) method in DMF solution are 113,000 and 863,000, respectively. Poly(methyl methacrylate) (PMMA; S10-001) was received from Cyro Industries. The average molecular weight of PMMA measured via solution viscosity is 110,000. As received, materials were dried in a vacuum oven at 80°C for at least 12 h to remove the moisture before the blending process and the subsequent injection-molding process. Blends of PVDF with PMMA were prepared by melt blending of the two components using a 30-mm JSW intermeshing co-rotating twin-screw extruder. The temperatures for seven zones on the extruder and the die were set to 196, 196, 198, 198, 198, 198, 198, and 200°C, respectively. The screw speed was kept constant at 90 rpm for all the blends prepared. Neat PVDF and PMMA were also extruded through the twin-screw extruder in order to keep the thermomechanical history the same for all the samples studied. The concentration of the blends are tabulated in Table I.

Injection Molding

The injection-molding process was performed on a Boy (Model 15S) 15-ton reciprocating-screw injection-molding machine equipped with a standard ASTM test mold and an oil-circulating mold temperature controller. The temperature of the mold surface was measured using a pyrometer, and the injection speed was determined using a linear variable differential transformer (LVDT), which monitored the forward motion of the screw relative to the barrel. The samples were prepared at two different mold temperatures (40 and 120°C) and at two different injection speeds (with the average injection flow rates of 6.9 and 34.5 cm^3/s, respectively). The rest of the processing variables, including melt temperature (195°C), injection pressure (13.8 MPa), back pressure (4.14 MPa), screw speed (165 rpm), and holding time (2 min) were kept constant. Large end-gated injection-molded tensile bars were selected for all the analysis.

Sample Sectioning

The geometry of the end-gated injection-molded sample bar is shown in Figure 1. Three cutting

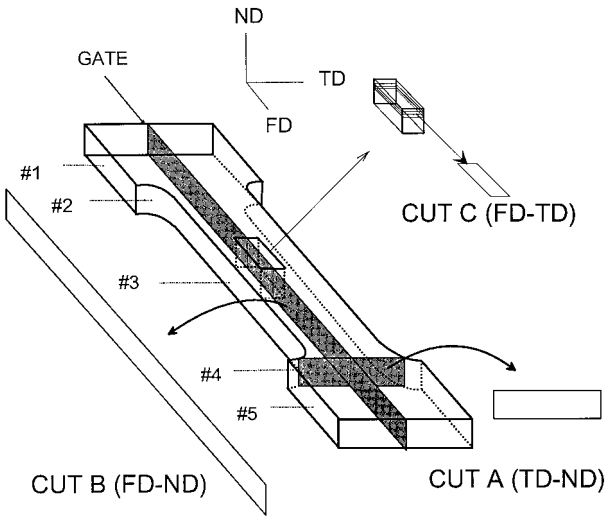

Figure 1 Schematics of cutting procedures (A), (B), and (C).

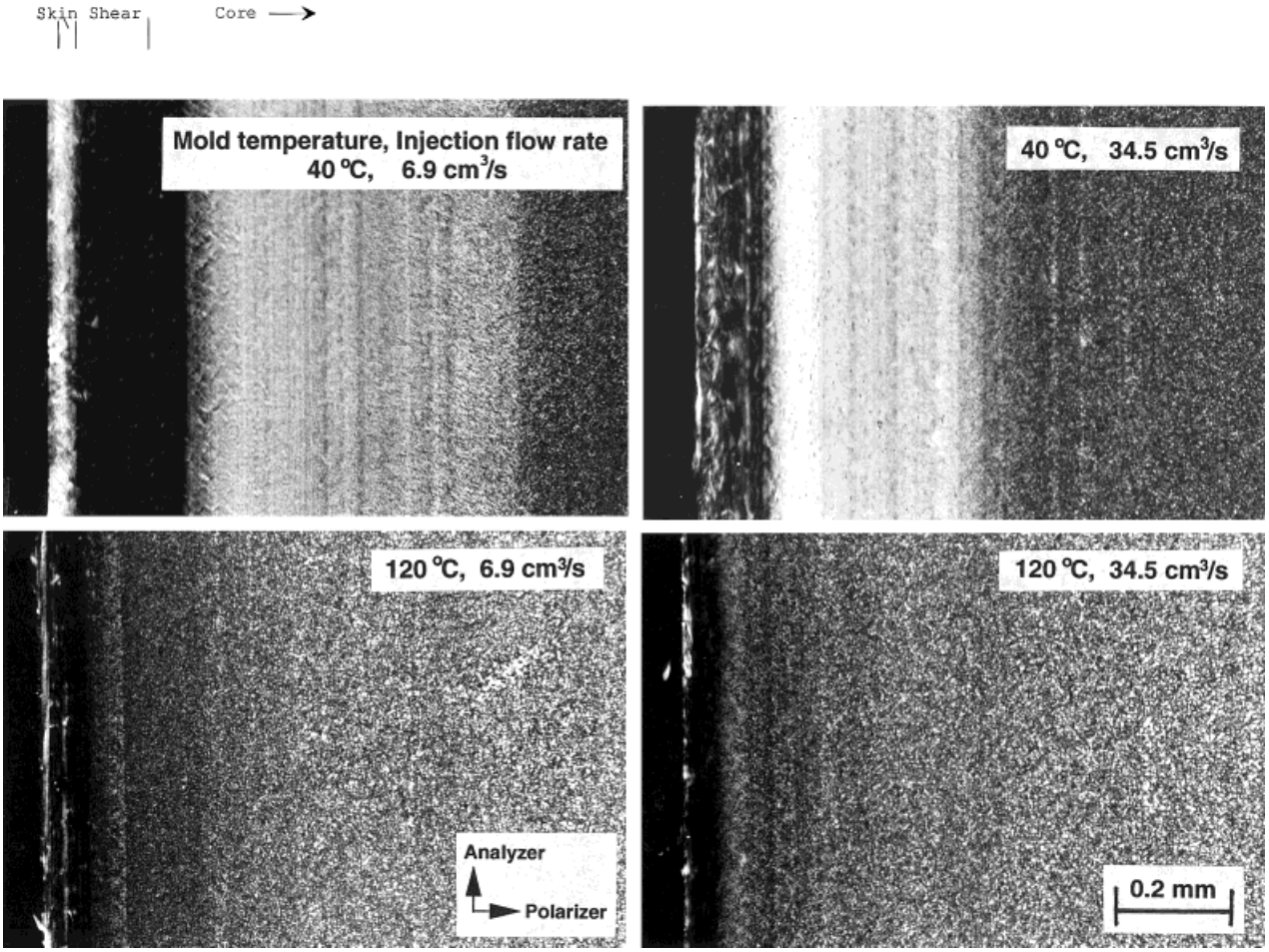

Figure 2 Optical micrographs (B-cut at #3 position) of PVDF samples molded at different conditions.

procedures were used to section the injection-molded samples: Procedure (A) consists of cutting sections in the TD-ND plane at #3 position perpendicular to the flow direction. In Procedure (B), the samples are sectioned in the mirror symmetry plane FD–ND along the flow direction. In procedure (C), the sample is cut from skin to core along the FD–TD plane at #3 position.

Thermal Analysis

The thermal analysis of the injection-molded PVDF and PVDF–PMMA blends at a series of locations from surface to core at position #3 (cutting procedure C, shown in Fig. 1) were performed using a DuPont DSC 910 apparatus. All samples were scanned at a heating rate of 20°C/min. The crystallinities of PVDF samples and the apparent crystallinities of the injection-molded blends of PVDF and PMMA were calculated using the following equations:

$$X(\%) = \frac{\Delta H_{\text{exp}}}{\Delta H^0} \times 100\% \quad (1)$$

$$\Delta H_{\text{exp}} = \Delta H_{\text{melt}} - \Delta H_{\text{cold cryt.}} \quad (2)$$

where ΔH^0 is the heat of fusion of 100% crystalline polymer. The value for PVDF is 104.7 J/g.[4] The true crystallinity in the PVDF portion was also calculated for injection-molded blends of PVDF with PMMA by dividing the apparent crystallinity by the PVDF concentration. This calculation was performed assuming a constant PVDF concentration at different locations from skin to core. Both the apparent crystallinity and the true crystallinity in the PVDF portion were plotted as a function of dis-

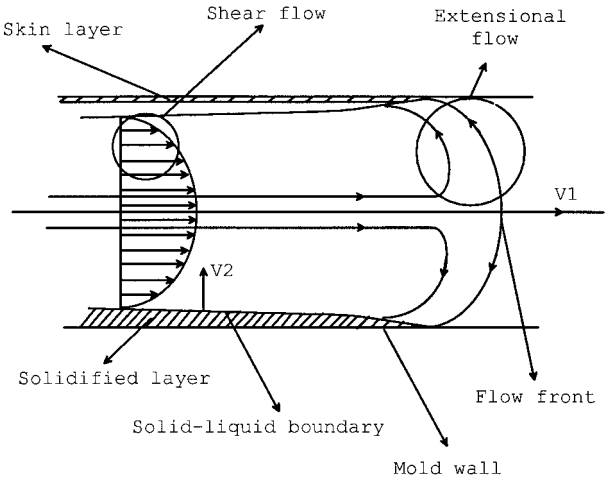

Figure 3 Schematic representation of the flow field in the mold cavity.

tance from the skin for the injection-molded blends of PVDF with PMMA.

In order to clarify the origins of multiple endothermic peaks observed in the differential scanning calorimetry (DSC) scans of the sample molded at the lower mold temperature (40°C), a DSC scan was also performed at a heating rate of 1°C/min on a slice of sample cut from the PVDF sample molded at 40°C mold temperature and at 6.9 cm^3/s injection flow rate. The slices were obtained by microtoming the sample at #3 position using the C-cut procedure shown in Figure 1. The slice in the core region was selected for this DSC study. Part of this slice was used in our thermal analysis using DSC, and the other part of the slice was used in our hot-stage polarized video microscopy study described below.

Optical Microscopy

The samples of about 20 to 30 μm thick were sliced from the injection-molded tensile bars using the cutting procedure (B) on a Reichert–Jung microtome (model 2050). They were then examined, and pictures were taken under cross polarizers using a Leitz Labolux 12 Pol S microscope. The thickness of each morphological layer was measured either directly on the microscope using a calibrated microscope eyepiece micrometer attachment or from the printed pictures.

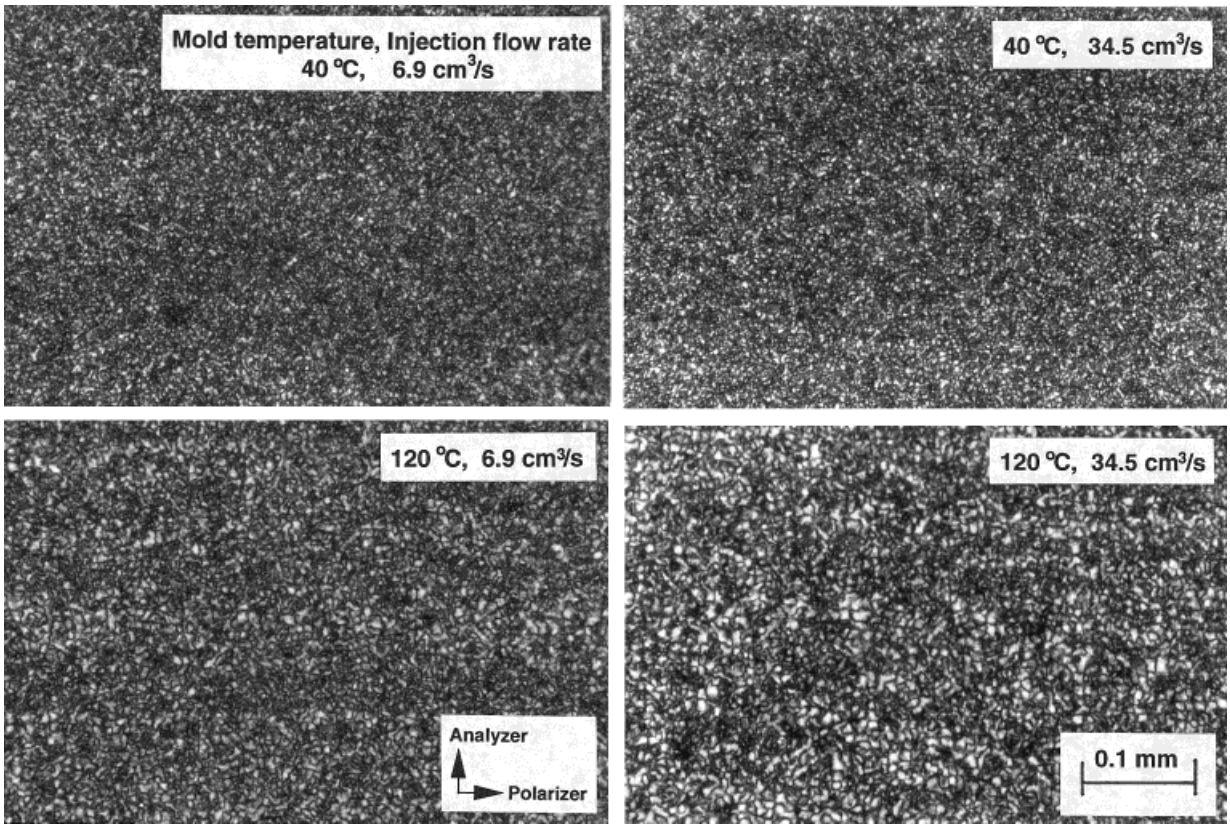

Figure 4 Cross-polarized optical micrographs (B-cut at the #3 position in the core) of PVDF samples molded at different conditions.

Table II Thickness of Each Morphological Layer in the Injection-Molded PVDF Samples at #3 Position

Molding Conditions (μm)	40°C, 6.9 cm^3/s	40°C, 34.5 cm^3/s	120°C, 6.9 cm^3/s	120°C, 34.5 cm^3/s
Skin layer	50	10	10	8
Shear zone	200	125	100	60
Core	1250	1365	1390	1432

Hot-Stage Polarized Video Microscopy

To identify the multiple endothermic peaks observed in the DSC scans, a Linkam hot stage (THM 600) was used to monitor the melting sequence of the PVDF sample molded at 40°C and at a 6.9 cm^3/s injection flow rate. The sample was cut at #3 position using the C-cut procedure shown in Figure 1. A slice of sample microtomed from the core of the sample was used for this study since the core has minimum level of molecular orientation and it shows clearly two melting peaks at a heating rate of 1°C/min. The heating scan was performed from 30 to 190°C at a heating rate of 1°C/min using the hot stage mounted on the polarized light microscope. The optical images at different temperatures were captured and converted to 8-bit gray-scale images using an image analysis system. The transmitted light intensity averaged over a large area at each temperature was then obtained using image analysis software. Since the experiment was performed under a cross-polarized light condition, the transmitted light intensity is a depolarized light intensity and roughly proportional to the crystallinity of the sample.[5] By tracing the transmitted light intensity as a function of temperature, one can monitor the crystallization and melting processes that take place at different temperatures.

RESULTS AND DISCUSSIONS

Optical Microscopy

Injection-Molded PVDF

Figure 2 shows the optical micrographs of PVDF samples cut using procedure (B) procedure (at the #3 position). It can be seen from this figure that all the samples molded under different injection-molding conditions possess a very similar three-layer morphology. The first layer is the skin layer formed as a result of the extensional flow that took place at the flow front before the material is solidified rapidly upon contact with the mold surface as shown in Figure 3. The second layer is the shear zone formed during cooling while the polymer chains experience considerable levels of shear flow. On the optical micrographs, this layer appears as a dark nonspherulitic band. The third layer is the spherulitic core. As expected, higher mold temperatures produce larger spherulites in the core regions as a result of decrease of cooling rates. The average size of the spherulites in the core is larger for the samples molded at the higher mold temperature (120°C) compared to the samples molded at the lower mold temperature (40°C), as shown in Figure 4. However, the size and the shape of the spherulites could not be determined as they are fairly small for quantitative measurements using optical microscope. In a separate study, we will report the spatial variation of crystal size and shape in injection-molded parts as determined by small-angle laser light scattering experiments.[6]

To quantitatively characterize the details of layer formations, we measured the thickness of each layer in injection-molded PVDF samples using optical microscopy. Table II shows the thick-

Table III Thickness of Each Morphological Layer at Different Positions in the PVDF Sample Molded at 40°C and at 6.9 cm^3/s Injection Flow Rate

Position	Skin Layer (μm)	Shear Layer (μm)	Core (μm)
Gate	45	200	1255
Convergence	50	200	1250
Center	50	200	1250
Divergence	50	150	1300
End	60	70	1370

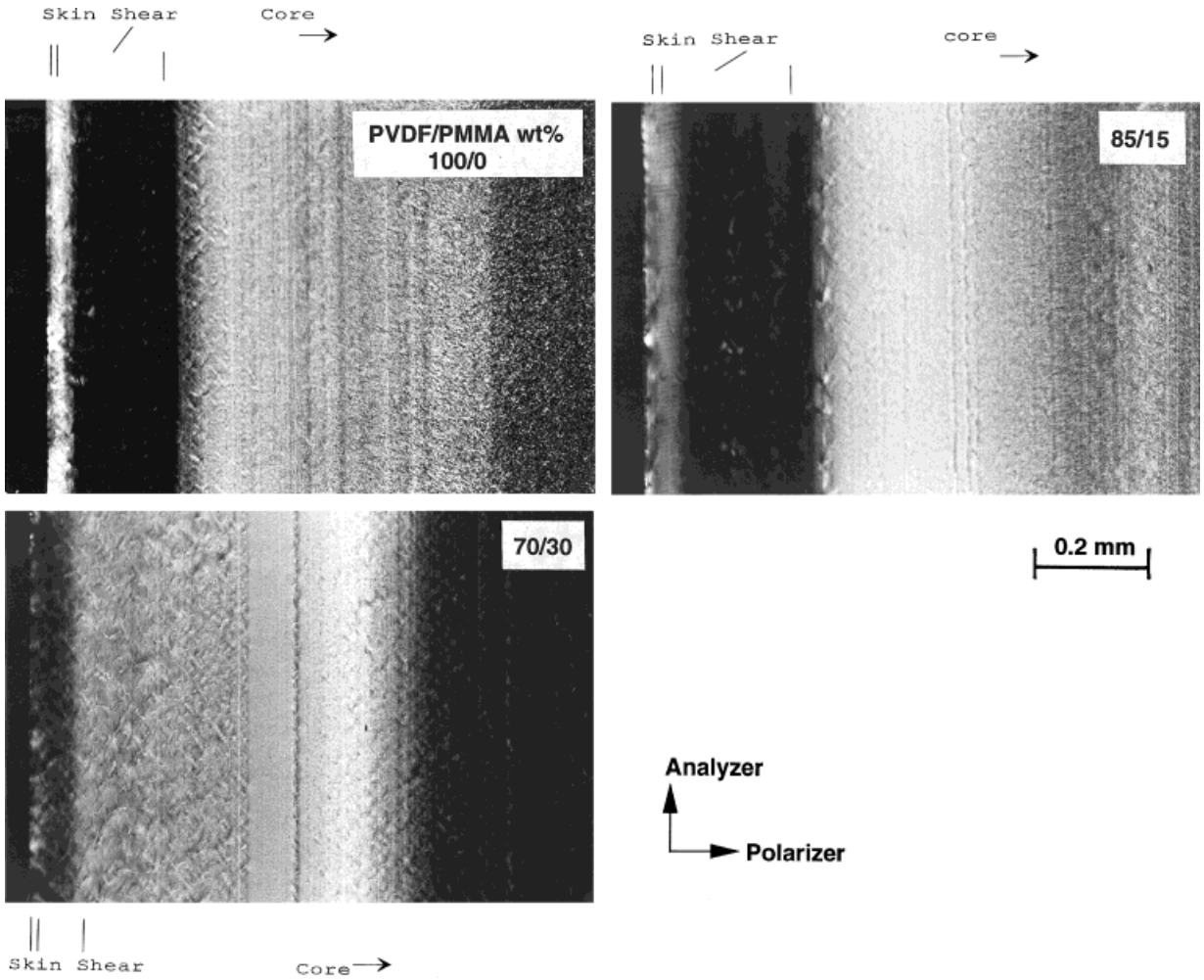

Figure 5 Cross-polarized optical micrographs (B-cut at the #3 position) of PVDF–PMMA samples molded at 40°C mold temperature and at 6.9 cm^3/s injection flow rate.

ness of each morphological layer in the samples molded under four different conditions. The samples molded at the lower mold temperature (40°C) has thicker skin layer and shear layer compared to the samples molded at the higher mold temperature (120°C) under the same injection speed. This can be explained with the help of Figure 3. During the injection-molding process, the flow front propagates at a velocity of V_1 while the solid–liquid boundary moves towards the core at a velocity of V_2. V_1 is fully controlled by the injection speed and, to a certain extent, by the rate of heat transfer in the thickness direction, which controls the given cross-sectional area that fluid passes through. The velocity of the movement of the solid–liquid boundary V_2 is controlled by the rate of heat transfer, which can only be changed either by changing the melt temperature or the mold temperature. At the lower mold temperature, the frozen layer (including shear zone) builds up faster (higher V_2) due to the higher rate of heat transfer through the wall. As a result, a thicker region of the material experiences high shear stress before the injection stage is completed. This is due to the higher V_2 and increased V_1 as a result of the reduction of the effective cross-sectional area by the increased thickness of the solidified layers. On the other hand, at the higher mold temperature, the material in the shear region may still be able to relax after the mold filling stage is completed and before the crystallization process starts. Therefore, we expect to see a thicker skin layer and shear zone for the sample molded at the lower mold temperature.

From Table II, we can also see the effect of injection speed on the morphology of the molded

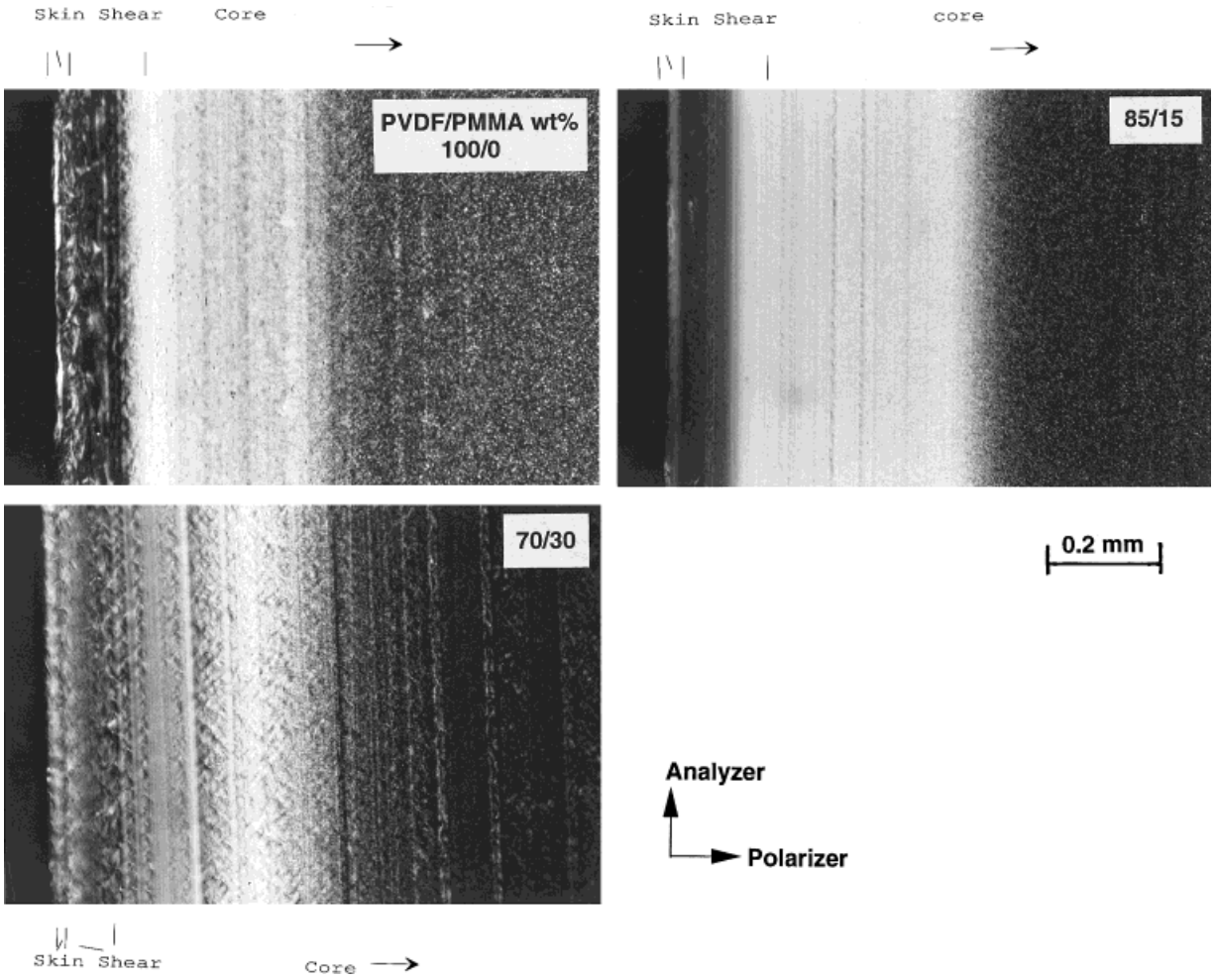

Figure 6 Cross-polarized optical micrographs (B-cut at the #3 position) of PVDF–PMMA samples molded at 40°C mold temperature and at 34.5 cm^3/s injection flow rate.

samples. In general, the higher the injection speed, the thinner the shear zone due to the composite effect of the following factors: The dominant factors influencing the formation of layers are the duration of time and temperature at which stresses are imposed onto fluid elements during the filling stage. At high injection speeds, the mold filling process is so fast that the material being sheared does not have sufficient time to cool down to temperatures at which thermal or stress induced crystallization occur. As a result, the built-up stresses can be relaxed, returning the polymer chains to a relatively unoriented state while the polymer melt temperature remains high enough not to start crystallization. When the crystallization eventually occurs as a result of cooling, the growth behavior becomes exclusively spherulitic. The effect of shear stress is thus less apparent and confined to regions that are closer to the mold wall at higher injection speeds. In contrast, at lower injection speeds, the material near the wall is exposed to high stresses for a longer period while the solidifying front immobilizes them in place forming much thicker layer. In brief, the overall morphology is determined by the composite effect of heat transfer (primarily heat loss through the part walls), shear stress, and molecular relaxation.

Secondly, at the lower injection speed, the frozen layer (skin plus shear layer) may build up at a speed comparable to the injection speed, especially at the low mold temperatures. As a result, the material injected at the lower injection speed experiences increased level of deformation history due to the reduction of the effective cross-sectional area. However, the shear

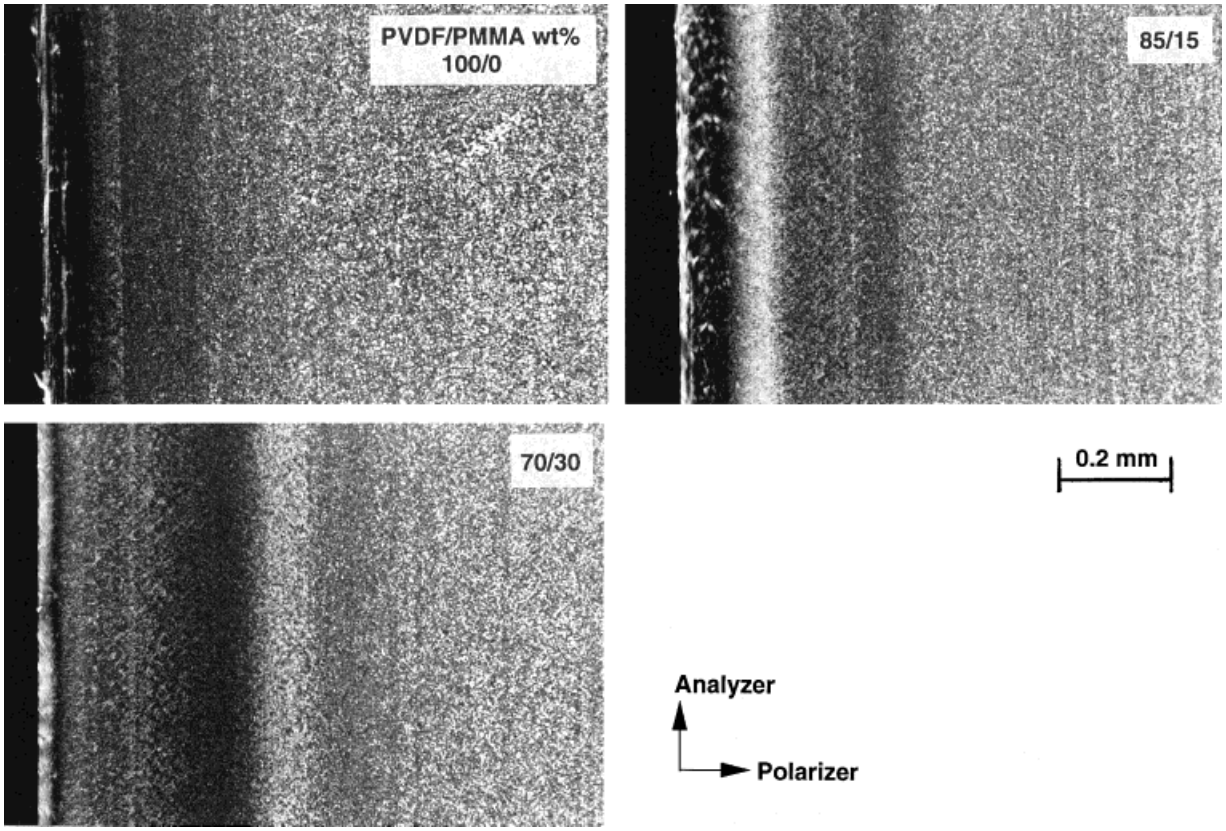

Figure 7 Cross-polarized optical micrographs (B-cut at #3 position) of PVDF–PMMA samples molded at 120°C mold temperature and at 6.9 cm^3/s injection flow rate.

zone is fairly thin compared to the overall thickness of the sample for almost all the samples molded. This clearly indicates that only a small fraction of polymer chains experience high stresses near the wall during the filling stage, and rapid relaxation of stresses at the interior of the parts produces mostly spherulitic regions. The very existence of spherulites in the core essentially confirms that whatever little stress levels that chains experience in these regions during filling eventually relaxes before the temperature becomes low enough for crystallization to occur. This means that the increase in the level of shear rate due to the reduction of the effective cross-sectional area may not be enough to reach the level of shear rates experienced at the higher injection speed. Thus, the influence of frozen layer advancement towards the core on the overall structural development becomes quite low.

In addition, at a higher injection speed, a higher level of shear stress may generate a higher level of heat in the nozzle and in the runner due to viscous heating. As a result, the temperature of the injected material in the cavity becomes higher than that of the material with the lower injection speed. In turn, the material injected with the higher injection speed may experience reduced a level of shear stress in the cavity due to the reduction of the viscosity resulting from the increase in the temperature, thereby compounding the effect.

The thickness of each morphological layer at different positions of the sample molded at 40°C and at 6.9 cm^3/s injection flow rate is shown in Table III. Generally, the skin layer is much thinner than the shear layer and the core. The thickness of the skin layer increases from 45 μm at the gate to 60 μm at the end of the tensile bar. In the convergence and center regions, the thickness of all the layers does not change. The thickness of the shear layer decreases drastically at the end of the tensile bar while the thickness of the skin and the core increases due to the reduced shear flow history experienced by the material in that region during crystalliza-

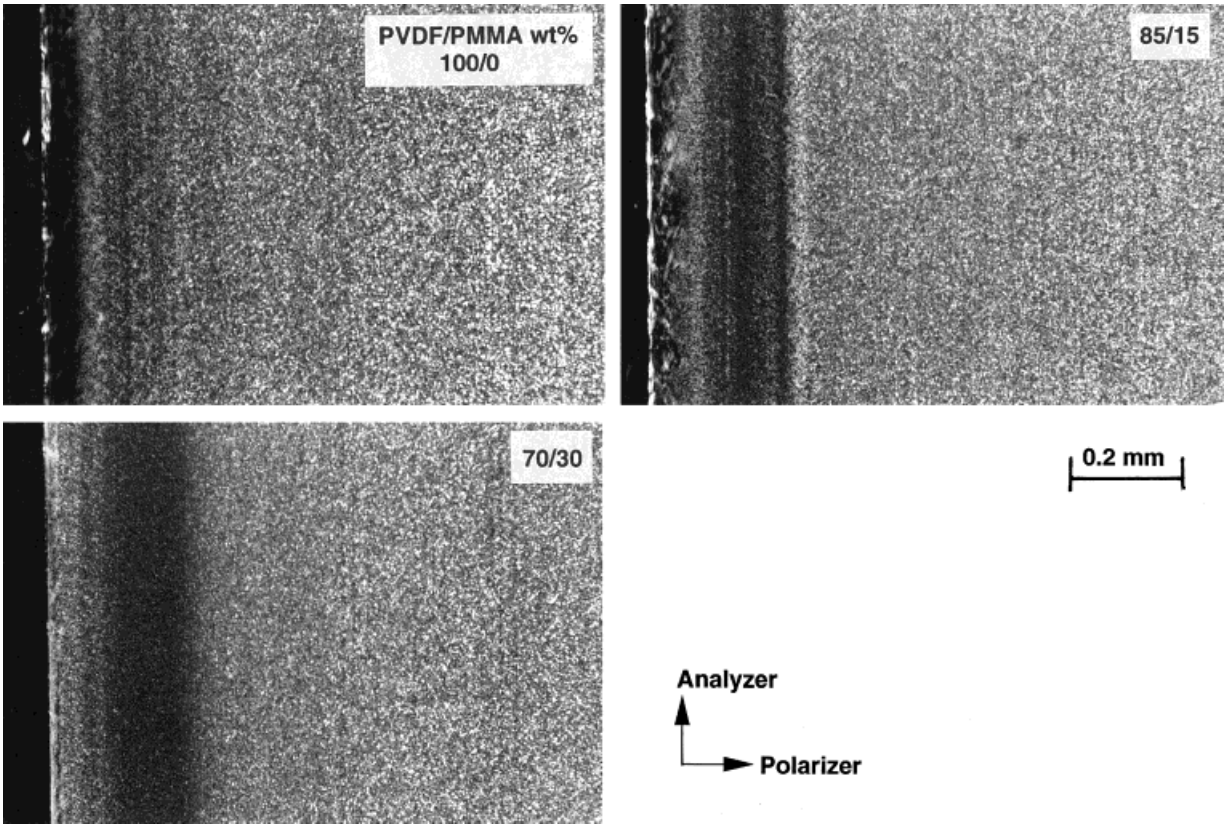

Figure 8 Cross-polarized optical micrographs (B-cut at #3 position) of PVDF–PMMA samples molded at 120°C mold temperature and at 34.5 cm^3/s injection flow rate.

tion. This is due to the rapid cessation of flow once the flow front reaches the end of the cavity.

Injection-Molded Blends of PVDF with PMMA

To study the effect of PMMA concentration on the morphology of the injection-molded blends of PVDF with PMMA, we also performed a similar morphological analysis on the injection-molded PVDF–PMMA blends using the optical microscope.

Figures 5 through 8 show the optical micrographs (at #3 position) of the blends molded under four different injection-molding conditions. These photomicrographs indicate that the addition of PMMA causes a significant reduction in the size of the spherulites. When PMMA concentration goes beyond 30 wt % in the blends, the spherulitic morphology is no longer observed in the core regions.

Figure 9 shows the thickness of each morphological layer versus PMMA content for the samples molded under four different injection-molding conditions. It can be clearly seen from this figure that the effects of injection-molding conditions on the layer thickness is much more pronounced than the dilution effect caused by the increase in PMMA concentration.

At the same mold temperature (40°C) and injection flow rate (6.9 cm^3/s), the thickness of the skin layer increases first (at 85 wt % of PVDF) and then decreases as the PMMA fraction increases. The thickness of the shear layer increases at the expense of the core layer with the increase of PMMA concentration. However, the boundary between the shear layer and the core under this injection-molding condition becomes diffuse when the PMMA concentration increases to a level above 30 wt %. This is as a result of decrease of crystallizability caused by the dilution effect of the atactic PMMA. Therefore, for 30 and 45% PMMA concentrations, the data for these layers are omitted.

The thickness of the skin layer of the sample molded at 40°C and at a 34.5 cm^3/s average injection flow rate increases first (at 85 wt % of PVDF) and then decreases as PMMA content increases.

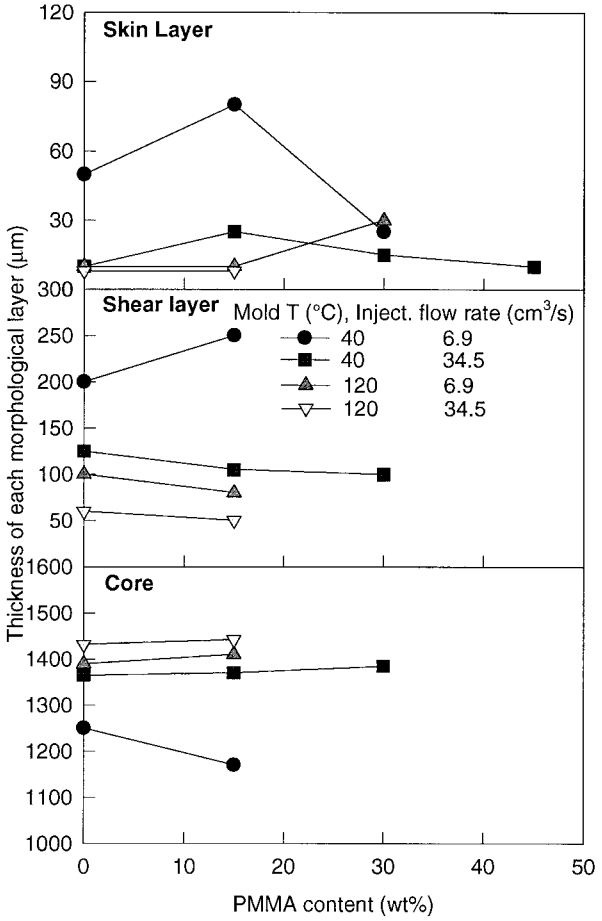

Figure 9 Thickness of each morphological layer for injection-molded PVDF–PMMA samples under different injection-molding conditions.

However, the thickness of the shear layer decreases continuously, which also increases the core region thickness.

The changes in the thickness of each morphological layer due to the changes in the blend compositions for blends of PVDF with PMMA do not follow a general trend. This, we believe, is partly due to unusual increases in the crystallization rates at a low concentration of noncrystallizable components. It was observed that the crystallization rates increase at small concentrations of the amorphous component before the dilution effect begins to take effect and reduce the rates of crystallization by increasing the average spatial separation distances between crystallizable chains (dilution effect). As summarized by Utracki,[7] there may be more than one reason for this effect, such as an increase of nucleation density at small concentrations or increased chain mobility. It is not likely that chain mobility is the case in our system as PMMA is much stiffer than PVDF.

In summary, the formation and the thickness of each layer is determined by a complex interplay between the thermal behavior and the rheological behavior of the blends and between the thermal history and the flow history imposed on the blends during the injection-molding process.

Differential Scanning Calorimetry

Injection-Molded PVDF

To investigate the thermal behavior of different layers from skin to core, a series of layers were sliced for each sample using cutting procedure (C), shown in Figure 1 at the #3 position, which is the midpoint between the two ends of the tensile bar. Figures 10 through 13 show the DSC thermograms of various layers from skin to core for parts molded at four different conditions. Most of these curves exhibit minor endothermic peak

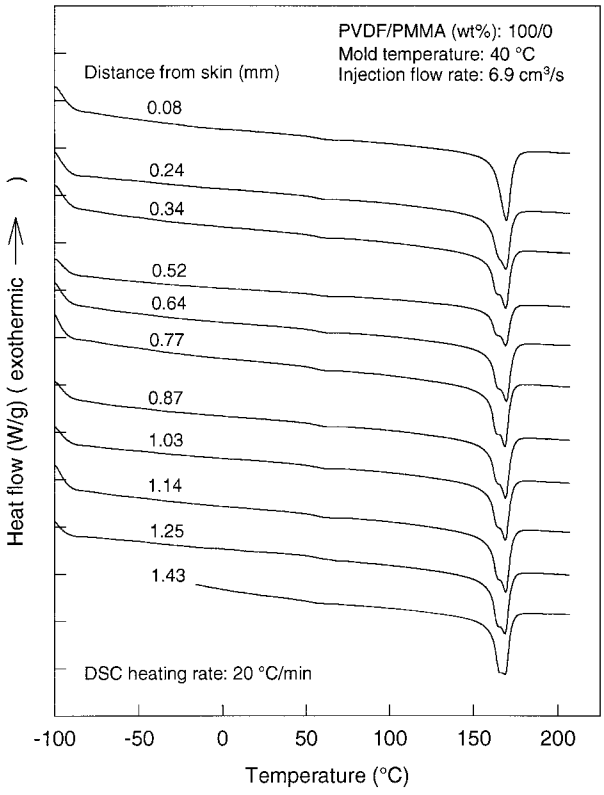

Figure 10 DSC thermograms of various layers of a PVDF sample molded at 40°C mold temperature and at 6.9 cm^3/s injection flow rate.

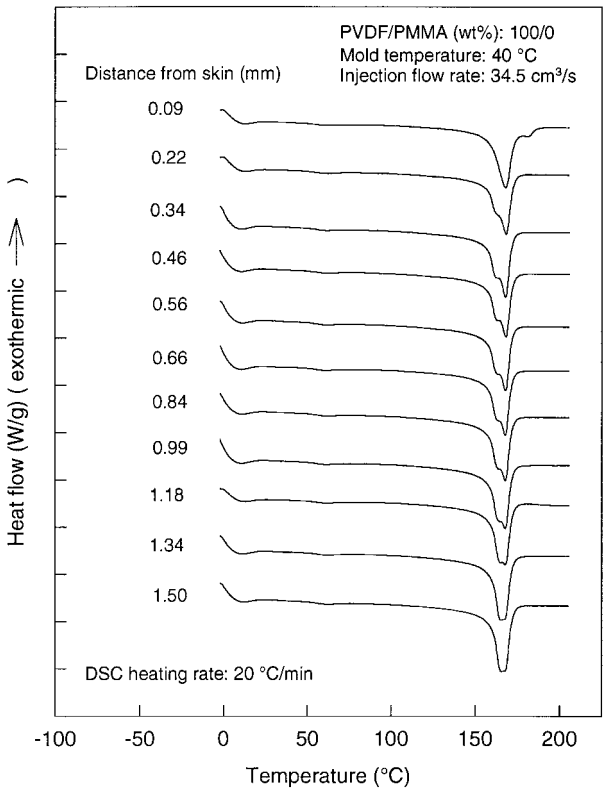

Figure 11 DSC thermograms of various layers of a PVDF sample molded at 40°C mold temperature and at 34.5 cm^3/s injection flow rate.

around 65°C. This is primarily as a result of aging of the samples stored at room temperature prior to testing. The samples rapidly quenched through T_g and reheated immediately afterwards in DSC did not show this peak.[8,9]

The samples molded at 40°C show two melting peaks in the temperature range from 150 to 175°C, except in the surface layers, where only one melting peak is observed (Figs. 10 and 11). These two melting peaks are fairly close to each other, and the lower melting peak gradually shifts towards the higher melting peak as the distance from the skin increases.

The appearance of the double melting peaks has been observed in many polymers. The origin of such phenomena has been discussed by many researchers.[10–14] One of the reasons is the melting of two distinct populations of crystals of different sizes as have been observed in poly(ethylene terephthalate)(PET)[15,16] and in annealed PVDF.[4] In fact, one can readily generate a series of melting peaks in most polymers by stepwise cooling from the melt. This results in a series of crystallite sizes of distinctly different melting temperatures. However, the melting endothermic doublet is not necessarily an indication of the bimodal distribution of crystalline melting points of the initial material as explained by Nichols and Robertson.[17] Todoki and Kawaguchi[18] demonstrated in their thermal analysis of Nylon 66 fibers that the pair of melting peaks could arise from an initial single peak crystal distribution that is undergoing melting, recrystallization, and remelting during an upward temperature scan. In addition, PVDF has several crystalline forms. Among them, the β crystals crystallized under certain conditions melt at a temperature higher than the normal melting temperature of the α crystals.[19] Thus, the appearance of the double melting peaks could also be due to the existence of two different crystalline phases. To find the origin of these melting peaks, other experiments such as wide-angle X-ray diffraction (WAXRD) and Fourier transform infrared (FTIR) need to be performed in conjunction with the hot-stage polarized video microscopy study.

It is also interesting to note that the sample

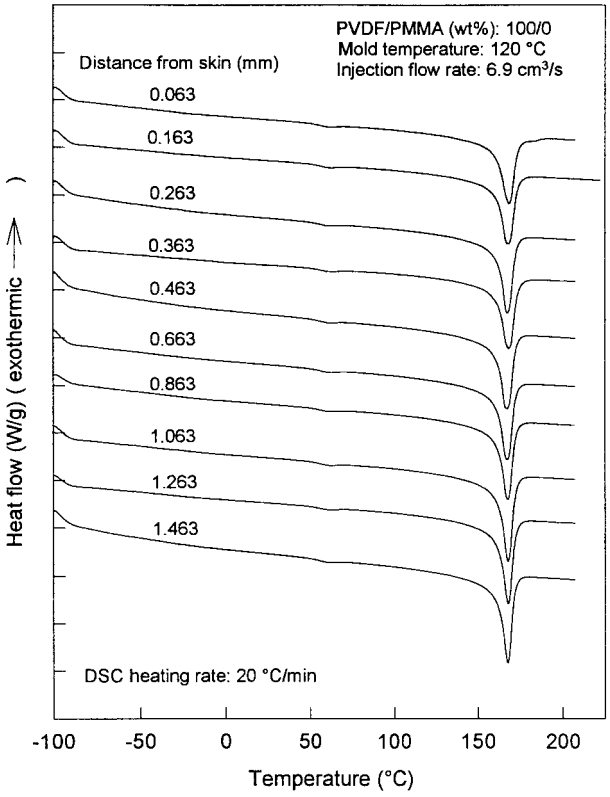

Figure 12 DSC thermograms of various layers of a PVDF sample molded at 120°C mold temperature and at 6.9 cm^3/s injection flow rate.

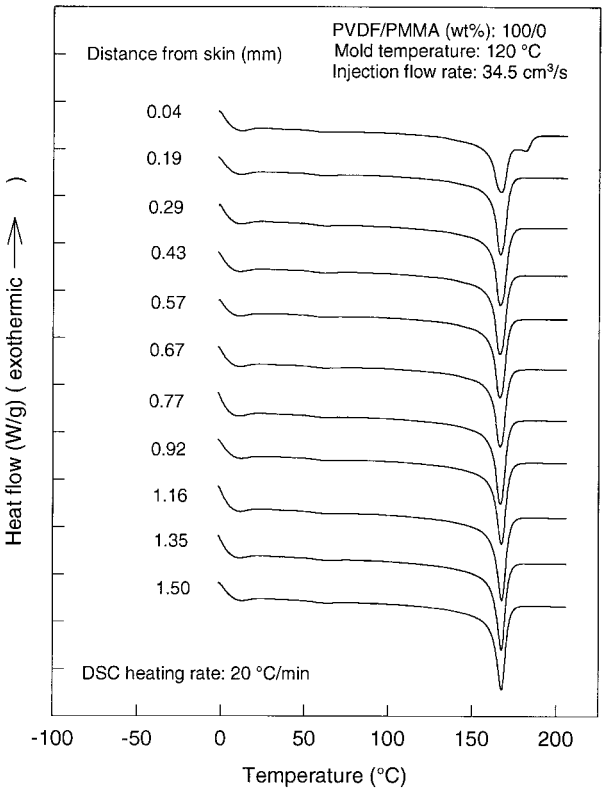

Figure 13 DSC thermograms of various layers of a PVDF sample molded at 120°C mold temperature and at 34.5 cm^3/s injection flow rate.

molded at 40°C and at a 34.5 cm^3/s injection flow rate shows an extra melting peak at a temperature (182°C) above the normal melting temperature range (150 to 175°C) in the surface layer. This extra melting peak is also present in the surface layers of the samples molded at 120°C, as shown in Figures 12 and 13. And, the area under this extra melting peak is much larger in the sample molded at the higher mold temperature (120°C) and a higher injection flow rate (34.5 cm^3/s). The existence of such a high temperature melting peak in the surface layer is related to the melting of the β crystals formed as a result of the fountain flow under the slower cooling rate, as will be discussed in a companion article.[20] In contrast to the samples molded at 40°C mold temperature, the samples molded at 120°C mold temperature show only one melting peak from skin to core in the normal melting temperature range (150 to 175°C). The differences in the thermal behavior between the samples molded under different conditions are due to the differences in the thermomechanical history that the material experiences during the injection-molding process.

More interestingly, the degree of crystallinity calculated based on the area under the melting peak does not change significantly from skin to core for all the samples as shown in Figure 14. The effect of shear stress on the final degree of crystallinity is absent on these samples, indicating a typical crystallization behavior of the fast crystallizing polymers.

The effect of injection-molding conditions on the crystallinity profiles can also be seen from Figure 14. The samples molded at the higher mold temperature (120°C) possess a relatively high overall level of crystallinities as compared to the samples molded at the lower mold temperature (40°C). This is primarily due to the increased role of thermally induced crystallization at the elevated mold temperature in developing the final structure. In these results, the degree of crystallinity was found to be relatively insensitive to changes in the injection speed.

Injection-Molded Blends of PVDF with PMMA

To study the influence of PMMA on the thermal behavior of the injection-molded blends, a series DSC tests was performed on the blend samples molded at 40 and 120°C mold temperatures with a lower injection flow rate (6.9 cm^3/s).

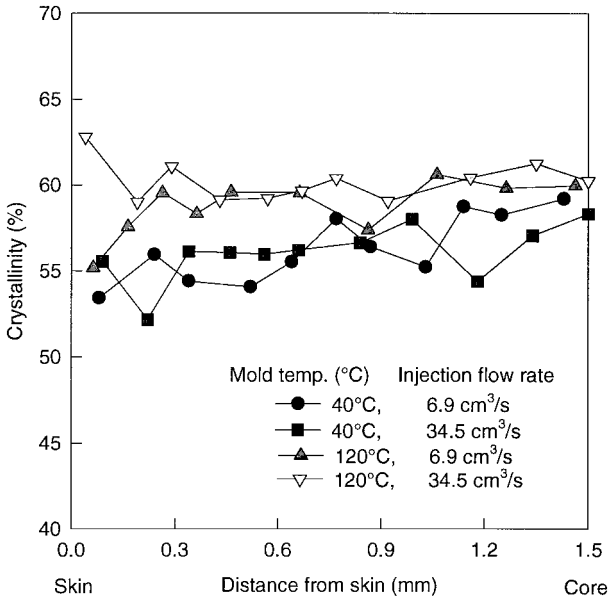

Figure 14 Crystallinity profiles at the #3 position (C-cut) for injection-molded PVDF samples obtained at different molding conditions.

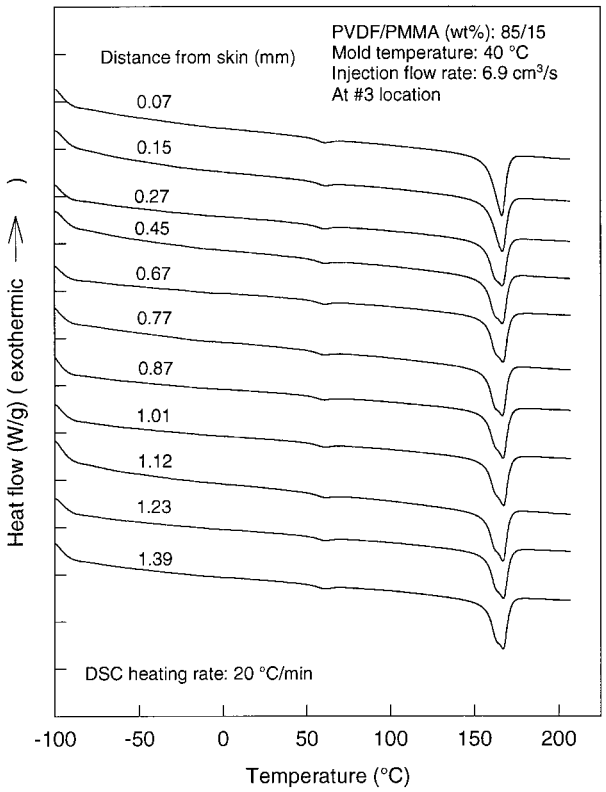

Figure 15 DSC thermograms of various layers of a PVDF–PMMA (85/15 wt %) sample molded at 40°C mold temperature and at 6.9 cm^3/s injection flow rate.

Figure 15 shows DSC thermograms taken at a series of depths from skin to core (#3 position) of the sample (85/15 PVDF–PMMA wt %) molded at 40°C mold temperature and at 6.9 cm^3/s injection flow rate. The core region of this sample shows double melting peaks very similar to those we have seen with the PVDF sample molded under the same injection-molding condition (Fig. 10). However, the melting peak positions shift slightly to the lower temperatures due to the depression caused by the addition of the PMMA component.

At the higher mold temperature (120°C) and at the lower injection flow rate (6.9 cm^3/s), the PVDF–PMMA sample (85/15 wt %) shows a similar DSC thermogram from skin to core with a single melting peak (Fig. 16). Similarly, the samples (70/30 wt %) molded under two different mold temperatures (40 and 120°C) show only one melting peak from skin to core (Figs. 17 and 18). However, the sample molded at the lower mold temperature (40°C) shows a much broader melting peak compared to the same blend molded at the higher mold temperature (120°C), suggesting the presence of a wider range of crystal sizes and/or imperfections.

When the PMMA fraction is increased to 45 wt %, the samples molded at two different mold temperatures (40 and 120°C) become amorphous across the thickness of the sample, as shown in Figures 19 and 20, respectively. On all these thermograms, in addition to the melting peak, a cold crystallization peak appears above the glass transition temperature. The presence of this peak represents crystallization during the DSC scan on heating the previously solidified material. Although this cold crystallization process irreversibly changes the structure of the original material, it carries an important information about the state of the polymer chains prior to heating. One is about the crystallizability of the chains. If the cold crystallization peak is present, it indicates that the polymer chains are crystallizable, and, as a result of specific thermomechanical history they experienced during their processing, they vitrified into a metastable noncrystalline state. Once sufficient thermal mobility is attained typi-

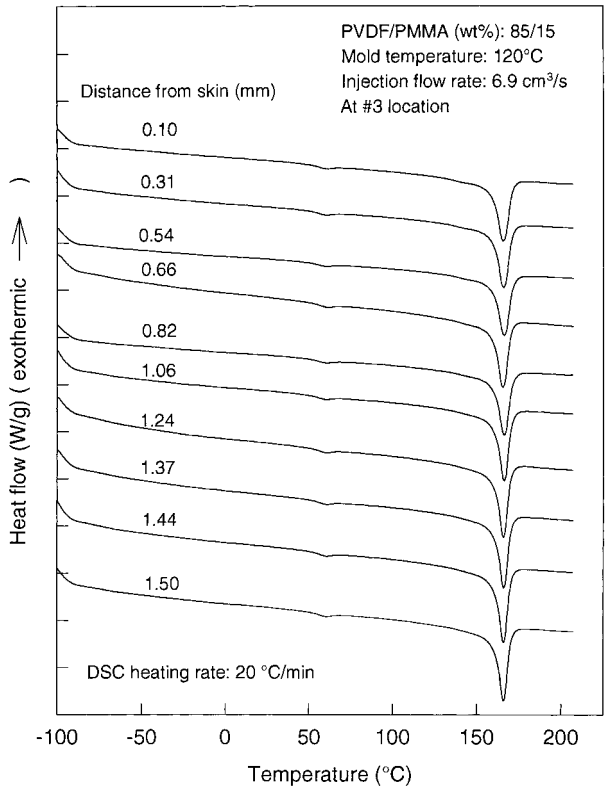

Figure 16 DSC thermograms of various layers of a PVDF–PMMA (85/15 wt %) sample molded at 120°C mold temperature and at 6.9 cm^3/s injection flow rate.

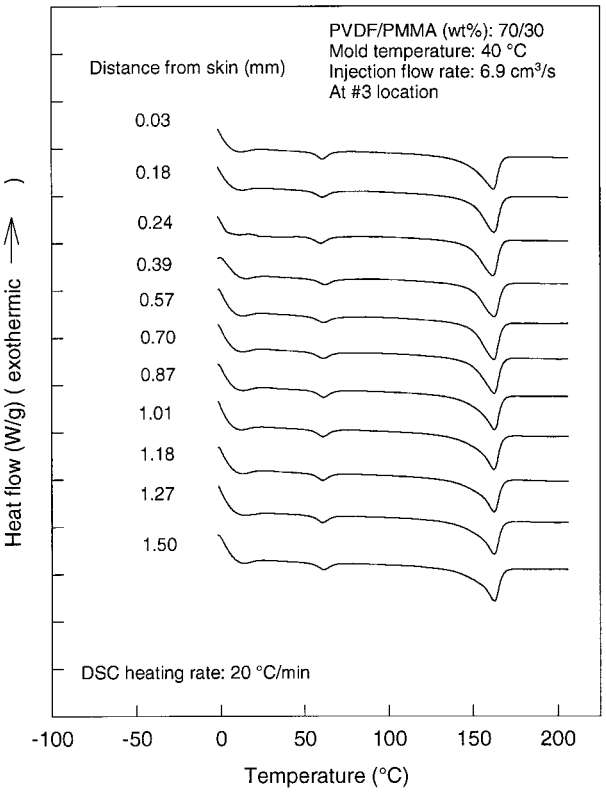

Figure 17 DSC thermograms of various layers of a PVDF–PMMA (70/30 wt %) sample molded at 40°C mold temperature and at 6.9 cm^3/s injection flow rate.

cally above the glass transition temperature, they crystallize. The second one is about the level of preferential orientation in the original material, which essentially dictates the temperature at which the peak position is observed. It was found in many polymeric systems that the higher the orientation level, the closer this peak position to the glass transition temperature. The reason for this is reduction of entropy by preferential orientation. As shown in Figure 21, the position of the cold crystallization temperature decreases, first reaching a minimum point in the depths where shear flow normally plays a role in structure formation, and then increases again, reaching a maximum point in the core. In the core, the cold crystallization temperature remains almost invariant for both of the samples tested. These results clearly indicate that PVDF chains in this composition can be vitrified into amorphous state under conditions typically encountered in injection molding. The polymer chains attain preferential orientation levels in the shear zone before vitrifying, and the subsequent heating essentially causes these regions to crystallize at lower temperatures as compared to the unoriented regions.

In addition, the results also indicate that the samples molded at the lower mold temperatures show a larger decrease in the cold crystallization temperature than the sample molded at the higher mold temperature due to the relatively higher level of molecular orientation in the shear layer of this sample. This is typical of slowly crystallizing polymers such as syndiotactic Polystyrene (SPS),[21] poly(ethylene naphthalate) (PEN),[22,23] and PEEK,[24,25] which, when processed from their quenched amorphous state, behave very much in this manner.

The effect of PMMA concentration on the crystallinities of PVDF–PMMA samples molded at two different mold temperatures is shown in Figure 22. The apparent crystallinity, as well as normalized true crystallinity, decreases significantly from skin to core as PMMA content increases. Like PVDF samples, PVDF–PMMA samples show a similar effect of the mold temperatures on the degree of crystallinity. The samples molded at the higher mold temperature (120°C) possess a higher overall level of crystallinity

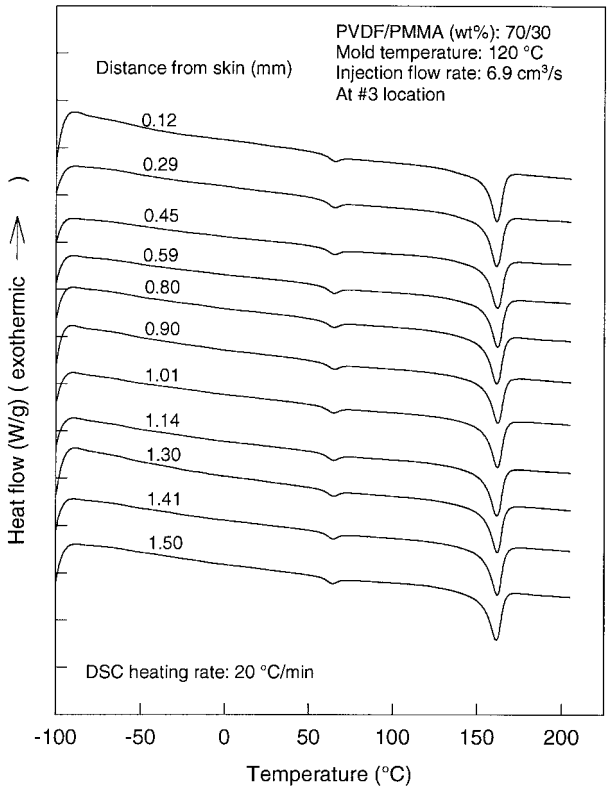

Figure 18 DSC thermograms of various layers of a PVDF–PMMA (70/30 wt %) sample molded at 120°C mold temperature and at 6.9 cm^3/s injection flow rate.

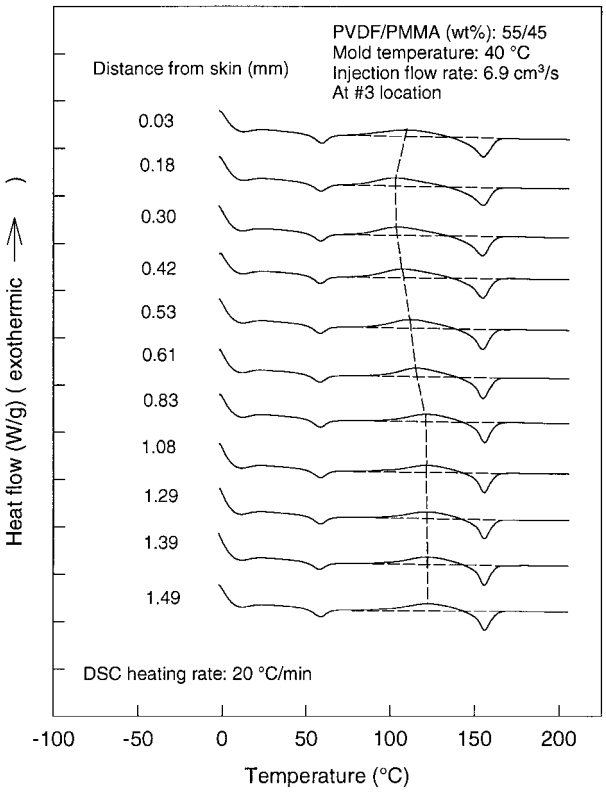

Figure 19 DSC thermograms of various layers of a PVDF–PMMA (55/45 wt %) sample molded at 40°C mold temperature and at 6.9 cm^3/s injection flow rate.

than the samples molded at the lower mold temperature (40°C). This is more apparent in the blends with 15 and 30 wt % of PMMA due to the increased dependency of thermal crystallization on the mold temperatures. As the PMMA content increases to 45 wt %, the samples molded at both higher and lower mold temperatures exhibit almost amorphous crystallinity profile (both apparent and true crystallinities) across the thickness as a result of the greatly reduced crystallizability and crystallization kinetics caused by the dilution of crystallizable PVDF chains by the noncrystallizable PMMA chains.

It is well known that the degree of crystallinity and the morphology of the molded parts are strongly dependent on the crystallization kinetics of the molded polymer. The injection-molded, slowly crystallizing polymers usually exhibit multilayered morphologies depending on the molding conditions. In the shear layer, these polymers tend to show an increased level of crystallinity due to the shear-induced crystallization process. It is thus expected that by controlling the crystallization kinetics by blending amorphous PMMA with PVDF, we can investigate the effect of shear stress on the morphology of the molded parts.

As shown in Figure 22, the degree of crystallinity (both apparent and true crystallinities) does not change significantly from skin to core for all the samples tested, including the blends with fairly slow crystallization kinetics. This indicates that the effect of shear stress on the final degree of crystallinity is minimal for these blends. Figure 22(a) shows the average crystallinity plotted against composition. It shows that crystallizability is abruptly diminished when the PMMA fraction increases beyond 30%.

One direct explanation for such an unusual behavior can be deduced from the crystallization behavior of the blends. When PVDF crystallizes, the PMMA chains have to be pushed away from the growth front of the PVDF crystals. Such a process greatly reduces the growth rate of the PVDF crystals. Under a high level of shear stress during the injection-molding process, the molecular chains are highly oriented, which puts them in a favorable situation to crystallize. However, the lateral

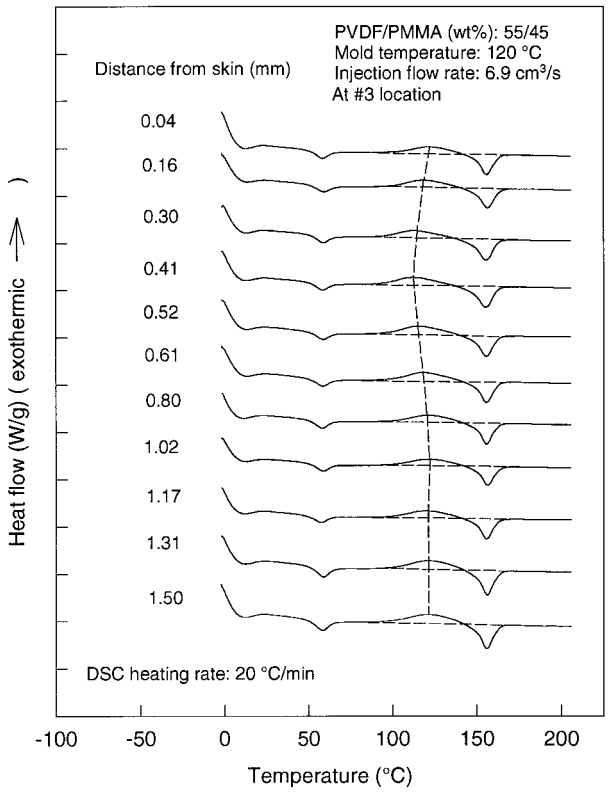

Figure 20 DSC thermograms of various layers of a PVDF–PMMA (55/45 wt %) sample molded at 120°C mold temperature and at 6.9 cm^3/s injection flow rate.

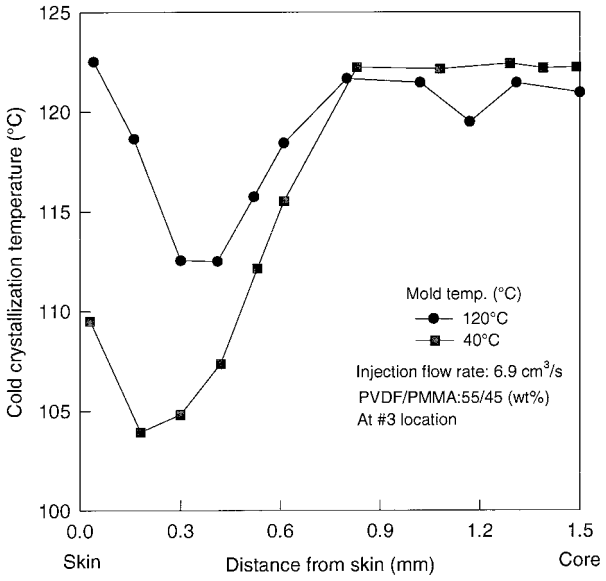

Figure 21 Cold crystallization peak temperature versus the distance from skin for an injection-molded PVDF–PMMA (55/45 wt %) blend at mold temperatures of 40 and 120°C.

diffusion of the PVDF chains to the growth front of the PVDF crystals is also reduced since both the PVDF chains and PMMA chains are aligned in the flow direction and they are under tension, which reduces the mobility of the PVDF and PMMA molecular chains in the other directions. As a result, the shear stress does not play a significant role on the final degree of crystallinity in these blends. If the liquid–liquid phase separation occurs before the crystallization under mechanical (stress) and/or thermal driving forces, one would clearly see the influence of stress history in crystallization behavior. If the phase separation is a result of crystallization, the process would be significantly slowed down by the diffusion limitation of the crystallization process, in which the noncrystallizable components would take their time to get out of the crystallization front. It appears that this phenomenon is partially linked to the forces that define the affinity of the two types of chains to one another, namely, the interaction parameter and its dependency on thermal deformation history. It appears that in this type of system, in which there is a strong

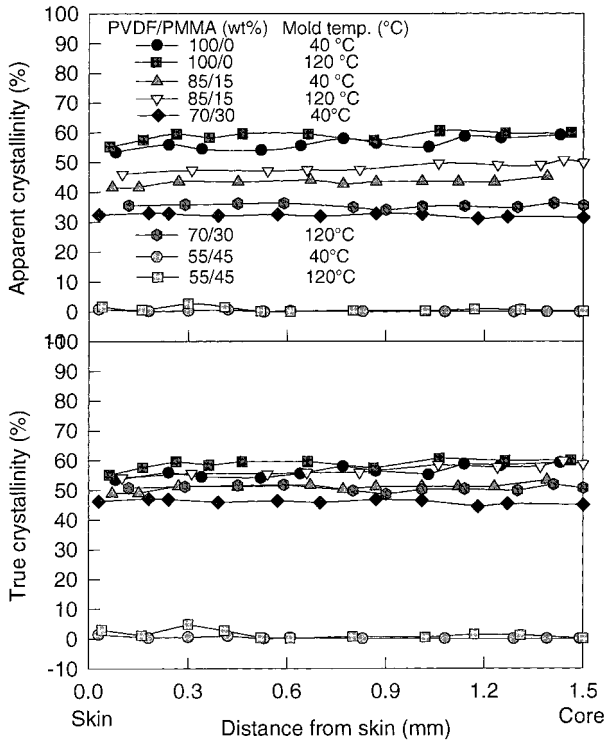

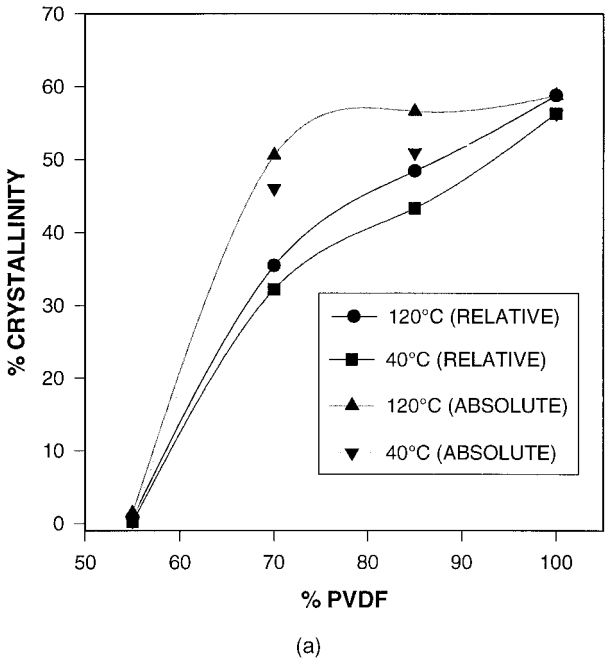

Figure 22 Crystallinity profiles at the #3 position (C-cut) for injection-molded PVDF–PMMA samples molded at 6.9 cm^3/s injection flow rate and at different mold temperatures. (a) Average crystallinity as a function of composition and mold temperature.

affinity between the two polymers (interaction parameter is strongly negative[8,26,27]), liquid–liquid phase separation is highly unlikely, even under the influence of high stress levels. Therefore, three-layer amorphous-skin-crystallized intermediate layer and amorphous core seen in other slowly crystallizing polymers, such as PPS,[28] PEEK,[24] PAEK,[29,30] PEN[22] is not observed; instead three-layer character appears in the graphs showing the spatial variation of the cold crystallization peaks where the shear effects are seen as the lowest temperature locations of the polymers. It is expected, however, that crystallization is still accelerated in the presence of shear stresses.

Hot-Stage Polarized Video Microscopy

As discussed before, the samples molded at the lower mold temperature (40°C) show two melting peaks in their DSC heating scans. To find the origin of these melting peaks, we performed a hot-stage polarized video microscopy experiment at a heating rate of 1°C/min on the slice cut from the PVDF sample molded at 40°C mold temperature and at a 6.9 cm^3/s injection flow rate. A DSC heating experiment was also performed at a heating rate of 1°C/min on the same sample in order to make comparison between the two experiments.

Figure 23(b) shows the transmitted light intensity obtained through the hot-stage polarized video microscopy experiment as a function of temperature. At about 125°C, the intensity of the transmitted light starts to decrease drastically with the increase of temperature due to the melting of the crystals. However, from this graph, we cannot clearly see if there exists a recrystallization process. This would have appeared as either change in the slope or temporary upturn in the intensity versus temperature curves.

Figure 23(a) shows the DSC thermograms of the same sample scanned at 1 and 20°C/min heating rates. As the heating rate is reduced from 20 to 1°C/min, the two melting peaks become well separated. The existence of the lower melting peak is probably due to the melting of the imperfect crystals formed during the fast cooling process, while the higher melting peak is due to the melting of more perfect crystals formed during the injection-molding process and also during the DSC heating process. The higher melting peak temperature increases from 168.3°C at a 20°C/min heating rate to 171.6°C at a 1°C/min heating rate. The area under the lower melting peak decreases and the area under the higher melting

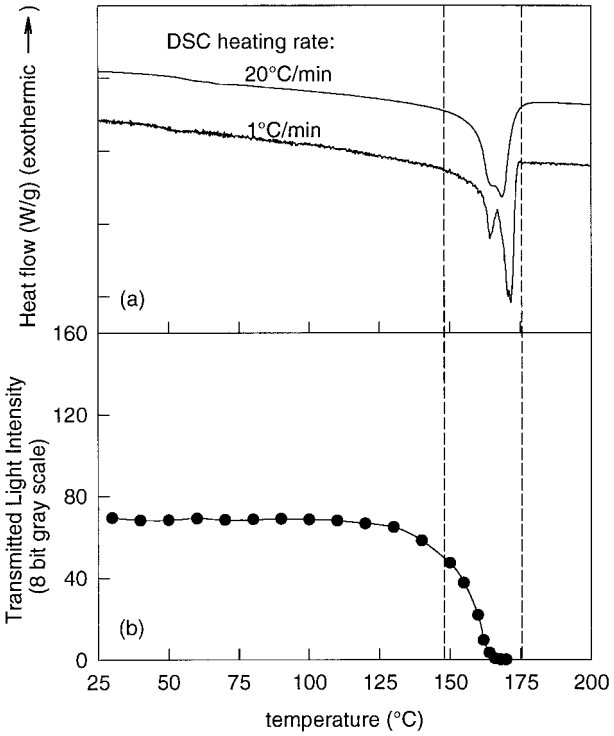

Figure 23 (a) DSC thermograms at two different heating rates for PVDF sample (40°C, 6.9 cm^3/s) at the #3 position in the core. (b) Transmitted light intensity versus temperature for the same sample tested at 1°C/min heating rate.

peak increases as the heating rate decreases. This indicates that the imperfect crystals go through melting, recrystallization, and remelting processes during the DSC heating scans. The imperfect crystals melt first and recrystallize into more perfect crystals during the heating process. Such a recrystallization process has been found in the DSC scan of polyimide 3,3′,4,4′benzophenonetetra carboxylic (dianhydride)–(2,2,dimethyl 1,3-(4-aminopbenoxy)-propane) (BTDA–DMDA)[31] and biodegradable poly-(3-hydroxybutyrate-*co*-3-hydroxyvalerate).[32–35] At the lower heating rate, the recrystallization process is more favored since the disordered crystals have enough time to melt and recrystallize into highly ordered crystals. Thus, the appearance of the higher melting peak is at least partially due to the melting of the recrystallized crystals during the DSC heating scans.

CONCLUSIONS

The injection-molded PVDF samples show typical three-layer morphology. The skin layer is formed under elongational flow. A second layer below this

is formed under the shear flow. The spherulitic core is developed mostly after the completion of the injection stage under little or no stress. The thickness of each morphological layer varies with changing processing conditions, such as the injection speed and the mold temperature.

The degree of crystallinity does not change significantly from skin to core for all the PVDF–PMMA samples molded under different molding conditions, indicating the absence of the stress-induced crystallization during the injection-molding process. This may be as a result of strong affinity of PVDF and PMMA chains to one another in the melt. This reduces the chance for a liquid–liquid phase separation, thereby limiting the crystallization process, even under high stresses. Other crystalline–noncrystalline polymers with less affinity to one another are expected to behave quite differently as they might exhibit a liquid–liquid phase separation before they crystallize under the influence of stress and thermal fields.

The DSC thermograms of the PVDF samples molded at the lower mold temperature show two melting peaks. The appearance of the lower temperature melting peak is due to the melting of the imperfect crystals formed during the fast cooling process. The existence of the higher melting peak is at least due partially to the melting of the crystals recrystallized during the DSC heating scans. The addition of PMMA results in a significant reduction in the overall level of crystallinity from skin to core due to the reduced crystallizability and reduced crystallization kinetics of the PVDF–PMMA blends.

Partial support for this research was provided by M. Cakmak's Presidential Young investigator Award from NSF DDM 8858303. The authors also thank the ELF Atochem North America and the Cyro Industries for supplying the polymers used in this study.

REFERENCES

1. J. P. Stallings and S. G. Howell, *Polym. Eng. Sci.,* **11,** 507 (1971).
2. J. P. Trotignon, J. Verdu, and R. Rogues, *Morphology of Polymers,* Walter de Gruyter & Co., Berlin, 1986, p. 297.
3. J. Mijovic, H. L. Luo, and C. D. Han, *Polym. Eng. Sci.,* **22,** 234 (1982).
4. K. Nakagawa and Y. Ishida, *J. Polym. Sci., Polym. Phys. Ed.,* **11,** 2153 (1973).
5. F. L. Binsbergen, *J. Macromol. Sci., Phys.,* **B4,** 837–852 (1970).
6. Y. D. Wang and M. Cakmak, *J. Appl. Polym. Sci.,* submitted.
7. L. A. Utracki, *Polymer Blends and Alloys: Thermodynamics and Rheology,* Hanser, NY, 1989, p. 61.
8. T. Nishi and T. T. Wang, *Macromolecules,* **8,** 909 (1975).
9. Y. Hirata and T. Kotaka, *Polym. J.,* **13,** 273 (1981).
10. H. Suzuki, J. Grebowicz, and B. Wunderlich, *Brit. Polym. J.,* **17,** 1 (1985).
11. Y. C. Lee and R. S. Porter, *Macromolecules,* **20,** 1336 (1987).
12. D. J. Blundell, *Polymer,* **28,** 2248 (1987).
13. S. Z. D. Cheng, *J. Appl. Polym. Sci., Appl. Polym. Symp.,* **43,** 315 (1989).
14. T. M. Chalmers, A.-Q. Zhang, D.-X. Shen, S. H.-S. Lien, C. C. Tso, P. A. Gabori, F. W. Harris, and S. Z. D. Cheng, *Polym. Int.,* **31,** 261 (1993).
15. R. C. Roberts, *Polymer,* **10,** 113 (1969).
16. R. C. Roberts, *Polymer,* **10,** 117 (1969).
17. M. E. Nichols and R. E. Robertson, *J. Polym. Sci., Polym. Phys. Ed.,* **30,** 305 (1992).
18. M. Todoki and T. Kawaguchi, *J. Polym. Sci., Polym. Phys. Ed.,* **15,** 1067 (1977).
19. Y. Wang, M. Cakmak, and J. L. White, *J. Appl. Polym. Sci.,* **30,** 2615 (1985).
20. Y. D. Wang and M. Cakmak, *J. Appl. Polym. Sci.,* submitted.
21. Y. Ulcer, M. Cakmak, C. Miao, and C. M. Hsiung, *J. Appl. Poly. Sci.,* **60,** 669 (1996).
22. Y. Ulcer and M. Cakmak, *Polymer,* **35,** 5651 (1994).
23. Y. D. Wang, M. Simhambhatla, and M. Cakmak, *Polym. Eng. Sci.,* **30,** 721 (1990).
24. C. M. Hsiung, M. Cakmak, and J. L. White, *Polym. Eng. Sci.,* **30,** 967 (1990).
25. M. Simhambhatla and M. Cakmak, *Polym. Eng. Sci.,* **35,** 1562 (1995).
26. J. H. Wendorff, *J. Polym. Sci., Polym. Lett. Ed.,* **18,** 439 (1980).
27. D. C. Douglass and V. J. McBrierty, *Macromolecules,* **11,** 766 (1978).
28. C. M. Hsiung, M. Cakmak, and J. L. White, *Int. Polym. Proc.,* **5,** 109 (1990).
29. C. M. Hsiung and M. Cakmak, *J. Appl. Polym. Sci.,* **47,** 125 (1993).
30. C. M. Hsiung and M. Cakmak, *J. Appl. Polym. Sci.,* **47,** 149 (1993).
31. Y. D. Wang, M. Cakmak, and F. W. Harris, *J. Appl. Polym. Sci.,* **56,** 837 (1995).
32. H. Mitomo, P. J. Barham, and A. Keller, *Polym. J.,* **19,** 1241 (1987).
33. A. J. Owen, J. Heinzel, Z. Skrbic, and V. Divjakovic, *Polymer,* **33,** 1563 (1992).
34. H. Mitomo, P. J. Barham, and A. Keller, *Sen-i Gakkaishi,* **42,** 45 (1986).
35. Y. D. Wang, T. Yamamoto, and M. Cakmak, *J. Appl. Polym. Sci.,* **61,** 1957 (1996).